Journal of Optoelectronics and Advanced Materials Vol. 7, No. 4, August 2005, p. 2085 - 2094

PREPARATION AND CHARACTERIZATION OF SnSe NANOCRYSTALLINE THIN FILMS

J. Sharma, G. Singh, A. Thakur, G. S. S. Saini, N. Goyal, S. K. Tripathi*

Centre of Advanced Study in Physics, Panjab University, Chandigarh-160 014, India

The present paper reports the preparation of nanocrystalline SnSe (n-SnSe) thin films by thermal evaporation of the material in the presence of a carrier gas. The normal incidence transmission spectra of the substrate with and without n-SnSe thin film have been recorded. The absorption coefficient (α) has been calculated using the transmission curve and the extinction coefficient (k) has been calculated using these values of α. Band gap (E_g) of thin film has been calculated from the plots of $(\alpha h\nu)^2$ vs hν. The value of the measured band gap has been utilized to calculate the crystallite size in the nanocrystalline film. The electrical measurements (dc conductivity and photoconductivity) have been done in the temperature range 295-350 K. DC conductivity (σ_d) measurement indicates that the conduction in this material is through an activated process having single activation energy in the investigated temperature range. Steady state photoconductivity (σ_{ph}) measurements have been done as a function of temperature (295-350 K) at intensity 1035 Lux. Transient photoconductivity measurements show that the decay of photocurrent is quite slow.

(Received July 4, 2005; accepted July 21, 2005)

Keywords: Nanocrystalline, Optical properties, Photosensitivity, Photoconductivity

1. Introduction

Semiconductor nanostructures are of current interest due to the variation of their bulk properties when their characteristic dimensions become smaller than the mean free path of the carriers [1-3]. A key aspect of semiconductors in a nanocrystalline thin film form is the modification of the energy levels and the density of states owing to the confinement of the charge carriers. The charge carriers are localized in nanocrystals and this leads to a blue shift in the band gap [4,5]. Semiconductor nanoparticles exhibit size-dependent electronic band gap energies [6], melting temperatures [7], soild-solid phase transition temperatures [8] and pressures [9]. These properties of nanocrystals make them an interesting category of materials from photovoltaic, photoelectrochemical, electrochemical and nanoelectronic devices point of view [10-13].

The physical properties of nanostructures are substantially influenced by the synthesis route and have a strong bearing on the structure and microstructure of the specimens. Preparation of nanomaterial samples, which are uniform in composition, size, shape, internal structure and surface chemistry, is essential to successfully mapping their size-dependent materials properties. These materials have been prepared by different techniques like low-pressure chemical vapour deposition (LPCVD) [14], dc/rf sputtering [15], molecular beam epitaxy (MBE) [16]. But these techniques are not very cost effective. Thermal evaporation of a material in the presence of a carrier gas is another technique, which is simple and less expensive. This technique has been utilized for the deposition of the metals and nanoclusters [17]. Nanocrystalline thin films of semiconductors have been the subject of intensive studies from fundamental, experimental and applied interests. Most of the studies have been done on II-VI and III-VI nanocrystalline materials. However, not much work has been reported in the IV-VI nanomaterials. Among the IV-VI compounds, tin selenide (SnSe) has potential

* Corresponding author: surya@pu.ac.in; surya_tr@yahoo.com

applications in memory switching devices, as efficient solar material and in holographic recording systems. So, the authors have decided to prepare thin films of SnSe in nanocrystalline form and to study its electrical and optical properties.

The present paper reports the application of the Ar carrier gas deposition method. n-SnSe thin films have been deposited at a partial pressure of ~ 10^{-2} mbar, which is much lower than the normal partial pressures used in the carrier gas deposition method. Optical measurements have been taken at room temperature (295 K) and the different parameters like absorption coefficient (α), extinction coefficient (k) and band gap (E_g) have been calculated. The steady state photoconductivity is studied as a function of temperature (295-350 K) at an intensity 1035 Lux. The intensity dependence of the photoconductivity is studied at 295 K. Transient photoconductivity measurements have also been carried out using white light at 295 K and at intensity 1035 Lux. Section 2 describes the experimental details. The results have been presented and discussed in section 3. The last section deals with the conclusions of this work.

2. Experimental procedure

The semiconducting Sn_6Se_{94} is prepared from its constituents (5N pure) by melt-quenching technique as described earlier [18]. Thin films of this material are prepared in a conventional vacuum coating system on well degassed Corning 7059 glass substrates. The substrates are cleaned chemically. Finally, the vapour cleaning with acetone and methanol is done. The substrates are heated at 120 ^oC to remove any moisture or methanol present. Thermal evaporation of the material is carried out from the Mo boat. These films are deposited at partial pressure of argon (~ 10^{-2} mbar). Before the deposition, the vacuum chamber is evacuated to a vacuum of 2 x 10^{-6} mbar. The Ar gas has been introduced into the chamber through specially designed inlet tube having a jet of diameter ~ 0.5 mm. This jet is kept adjacent to the evaporation boat pointing towards the glass substrates. The vacuum chamber is purged several times with spectroscopic grade Ar gas to remove any residual gas impurities. Finally, SnSe is evaporated at Ar gas pressure of 10^{-2} mbar. The distance between the source and the substrates is kept at 7 cm.

To study the optical properties of n-SnSe thin film, the transmission spectrum has been recorded using a double beam UV/VIS/NIR spectrometer [Hitachi-330] in the transmission range 400-2000 nm. The electrical measurements of these thin films has been carried out in a specially designed metallic sample holder where the heat filtered white light (200 W tungsten lamp) can be shown through a transparent quartz window. A vacuum of about 10^{-3} mbar is maintained throughout these measurements. Light intensity is measured using a digital luxmeter (Testron, model TES-1332). A planar geometry of the film (length ~ 1.0 cm; electrode gap ~ 8 x 10^{-2} cm) is used for the electrical measurements. Thick In electrode has been used for the electrical contacts. The thickness of the film is ~ 1000 Å. The photocurrent is obtained after subtracting the dark current from the current measured in the presence of light. For transient photoconductivity measurements, light is shone on the thin film and the rise in photocurrent is noted manually from a digital picometer (DPM-111 Model). The accuracy in I_{ph} measurements is typically 1 pA.

3. Results and discussion

3.1 Optical properties

Optical studies are obtained by recording the transmission spectra of the film deposited on glass substrate after subtracting the transmittance of the glass substrate as reference. Figure 1 shows the thin film-substrate system used for the optical measurements. The n-SnSe film has a thickness (d) and a complex refractive index $n^* = n - i\,k$, where n is the refractive index and k the extinction coefficient. The substrate is considered transparent ($k_s = 0$) and its refractive index is n_s. So, as suggested by J. N. Hodgson [19], the reflection coefficients, R_1 and R_2, and transmission coefficients T_1 and T_2 for the two interfaces, air-film and film-substrate respectively, are given by the following expressions

$$R_1 = \frac{(n-1)^2 + k^2}{(n+1)^2 + k^2} = 1 - T_1, \qquad R_2 = \frac{(n-n_s)^2 + k^2}{(n+n_s)^2 + k^2} = 1 - T_2 \tag{1}$$

T is the optical transmission for the film in the semi-infinite substrate approximation. For the film-substrate systems, we have measured *T* compared with the optical transmission of a glass substrate.

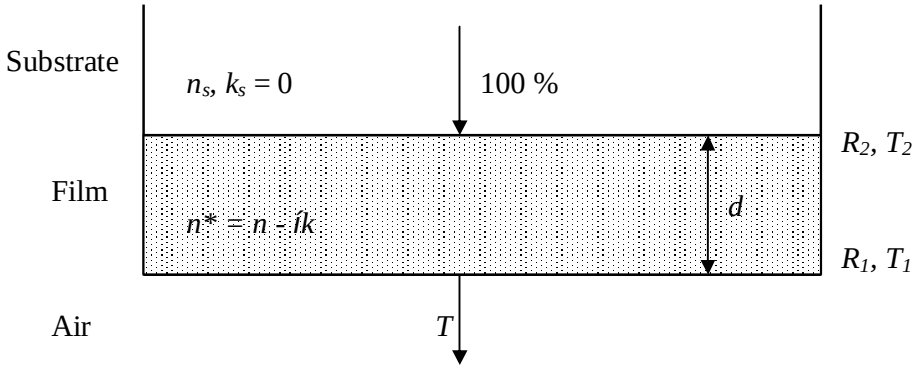

Fig. 1. Schematic representation of film-substrate system.

For a constant film thickness, the transmission coefficient (*T*) and the reflection coefficient (*R*), taking into account multiple reflections and interface effects, are given by Ynping *et al.* [20]

$$T = \frac{T_1 T_2 \tau}{1 - 2\sqrt{R_1 R_2}\,\tau \cos\varphi + R_1 R_2 \tau^2} \tag{2}$$

$$R = \frac{R_1 - 2\sqrt{R_1 R_2}\,\tau \cos\varphi + R_2 \tau^2}{1 - 2\sqrt{R_1 R_2}\,\tau \cos\varphi + R_1 R_2 \tau^2} \tag{3}$$ where

$\tau = exp\,(-\alpha d)$, $\alpha = 4\pi k/\lambda$ (absorption coefficient) and $\varphi = 4\pi nd/\lambda$. If $2nd = m\lambda$, where m is an integer (half integer), a maximum (minimum) in the transmission spectra is obtained. Percentage transmission (T %) as a function of wavelength (λ) for n-SnSe thin film is shown in Fig. 2.

From the transmittance data, nearly at the fundamental absorption edge, the absorption coefficient (α), are calculated in the region of strong absorption using the relation

$$\alpha = \frac{1}{d} \ln\left(\frac{1}{T}\right) \tag{4}$$

Using equation (4), the value of α has been calculated. Fig. 3 shows the plot of α vs photon energy. Using these values of α, the values of extinction coefficient (k) have been calculated and are plotted in Fig. 4. The fundamental absorption, which corresponds to the transition from valence band to the conduction band, can be used to determine the band gap of the materials. The relation between absorption coefficient (α) and the incident photon energy ($h\nu$) can be written as [21]

$$\alpha = \frac{A(h\nu - E_g)^n}{h\nu} \tag{5}$$

where *A* is a constant, E_g is the band gap of the material and the exponent n depends on the type of transition. n may have values 1/2, 2, 3/2 and 3 corresponding to the allowed direct, allowed indirect, forbidden direct and forbidden indirect transitions, respectively.

In case of nanocrystalline films, there may be some deviation from a bulk like transition. Now equation (5) may be written as

$$\frac{d\{\ln(\alpha h\nu)\}}{d(h\nu)} = \frac{n}{(h\nu - E_g)} \tag{6}$$

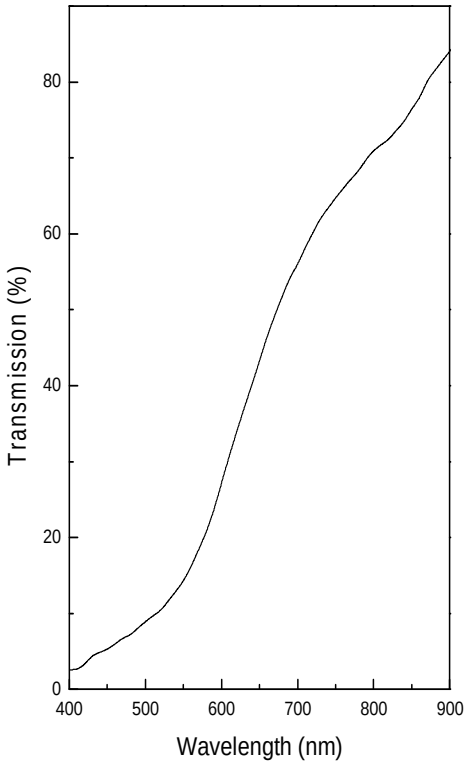

Fig. 2. Transmission spectra of n-SnSe thin film.

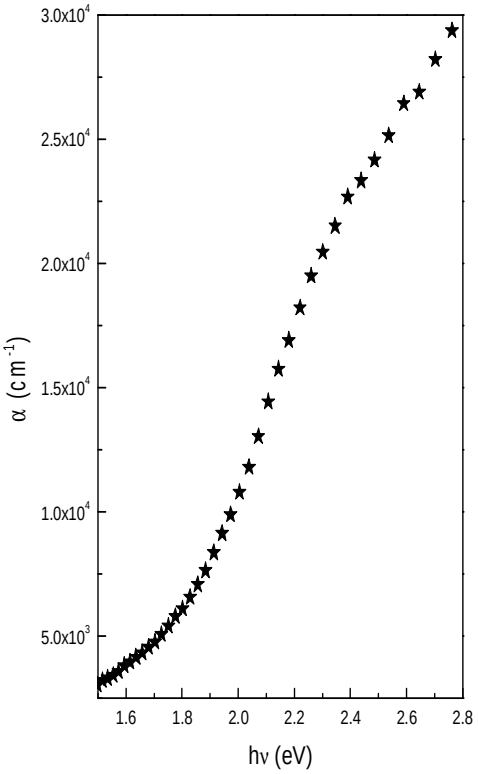

Fig. 3. Absorption coefficient of n-SnSe thin film.

The above equation indicates that the plot of d{ln(*αhν*)}/d(*hν*) vs *hν* must have a divergence at an energy value equal to E_g, where the transition takes place. Fig. 5 shows the plot of d{ln(*αhν*)}/d(*hν*) vs *hν*. We can see a discontinuity at 2.10 eV. Taking this value as the band gap of n-SnSe thin film, ln (*αhν*) vs ln ($h\nu - E_g$) graph is plotted, so that the nature of the transition (i.e. n value) can be determined. From the slope of this straight line graph (inset Fig. 6), value of n has been calculated, which is found to be 0.49 indicating that the transition is direct. Using this value of n (0.5), the exact value of the band gap is calculated by extrapolating the straight line portion of the $(\alpha h\nu)^{1/n}$ vs *hν* graph to the *hν* axis. Figure 6 shows the plot of $(\alpha h\nu)^{1/2}$ vs *hν*. The correct value of the band gap is found to be (2.18 ± 0.01) eV. It is observed that the value of E_g is higher than the bulk value of SnSe [(1.68 ± 0.01) eV] due to quantum confinement in the SnSe nanocrystallites. The bulk value of band gap is calculated from the transmission data of SnSe thin films deposited without the Ar carrier gas and pressure ~ 2 x 10^{-6} mbar.

From the blue-shift of the band gap (E_g), we can calculate the average diameter of the particles using relation [22,23]

$$\Delta E_g = E_g(film) - E_g(bulk) = E_{shift} = \frac{\hbar^2 \pi^2}{2\mu R^2} \tag{7}$$

where E_{shift} is the shift in the band gap, μ the translation mass (m_{hole} + $m_{electron}$) and *R* the radius of the nanoparticles. This formula is applicable in our case as we are well below the strong confinement

regime and hence observe the effects due to weak confinement of the exciton only. We have calculated the diameter of the nanoparticles using equation (7) and is found to be ~ 3 nm.

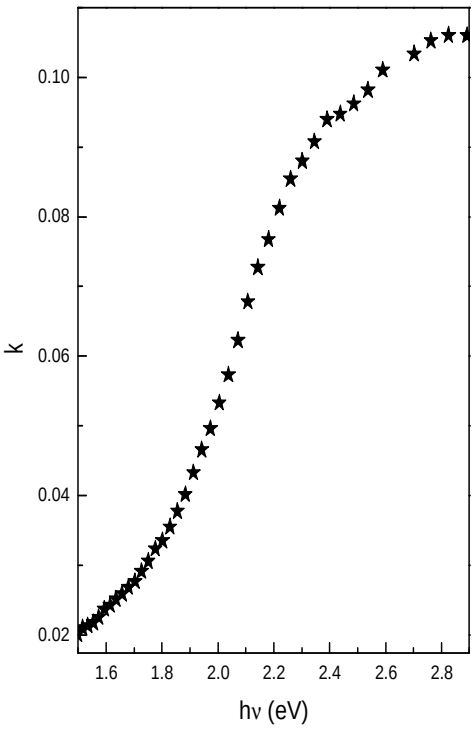

Fig. 4. Extinction coefficient at different energies for n-SnSe thin film.

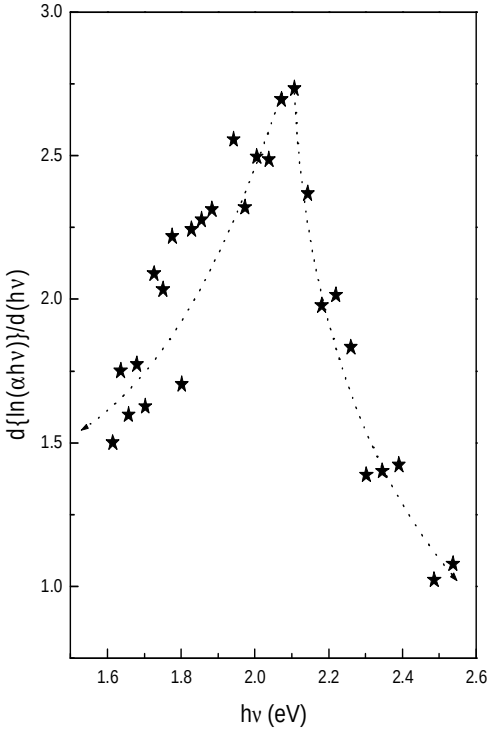

Fig. 5. Plots of d{ln(*αhν*)}/d(*hν*) vs *hν* for n-SnSe thin film.

In our case, the particle size decreases as the films are deposited in the presence of Ar partial pressure. This is in contrast with the behavior reported in literature [17,24] for depositions done in the carrier gas partial pressure at ~ 100 mbar, where the particle size is increased due to the increasing partial pressure. However, Chandra *et al*. [25] have observed a decrease in the particle size due to the increase in the Ar partial pressure. These contradictions can be explained from the behaviour of the vapour phase atoms in the different pressure regimes. In both cases, the cooling of vapours is through collisions with the carrier gas molecules, leading to the formation of small clusters in the gas phase. The partial pressure of the carrier gas governs the average size of these clusters, the higher the partial pressure, the smaller the cluster size. In the low pressure regime as in our experiment, the mean free paths being larger, the small clusters once formed, do not have further interaction with each other and are deposited directly on the substrate. In cases of CuCl and Ge nanoparticles [17,24] (in the high pressure regime), due to the smaller mean free paths, the clusters that are initially formed are slowed down substantially and in due course coalesce with each other. Due to this, formation of clusters takes place with bigger particle size as the partial pressure increases. These larger clusters eventually get deposited on the substrate.

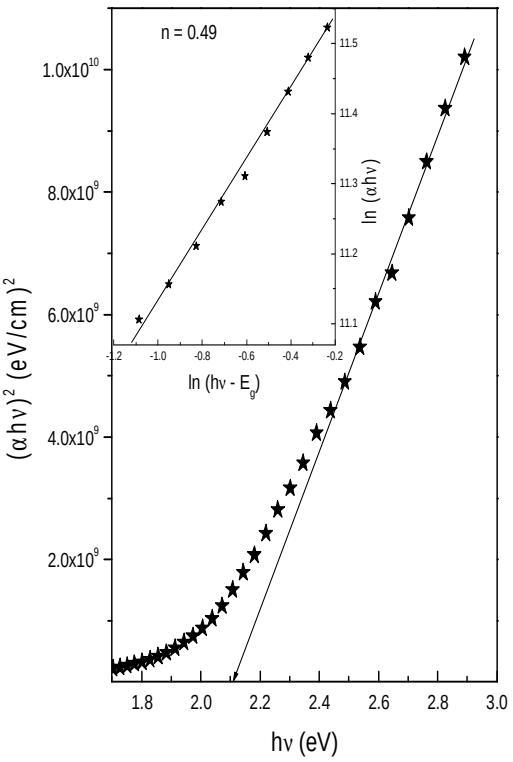

Fig. 6. Plot of $(\alpha h\nu)^2$ vs $h\nu$ for n-SnSe thin film. Inset: plot of ln $(\alpha h\nu)$ vs ln$(h\nu–E_g)$.

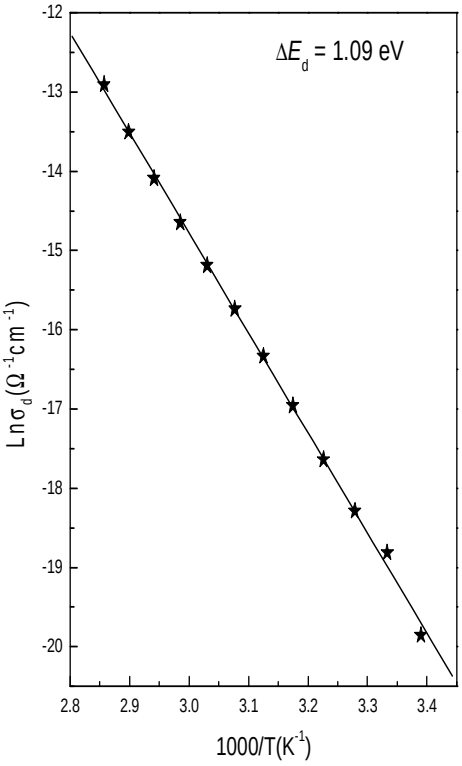

Fig. 7. Temperature dependence of dark conductivity for n- SnSe thin film.

3.2 Electrical measurements

3.2.1 Steady state photoconductivity

Fig. 7 shows the temperature dependence of dark conductivity (σ_d) for the thin films of n-SnSe. The plot of lnσ_d vs 1000/T is straight line indicating that conduction is an activated process having single activation energy in the temperature range 295-350 K. Therefore, σ_d can be expressed by the usual relation

$$\sigma_d = \sigma_o \exp\left(\frac{-\Delta E_d}{kT}\right) \tag{8}$$

where ΔE_d is the activation energy for dc conduction and k is the Boltzmann's constant. The value of ΔE_d is obtained from the slope of the plot of Fig. 7. The value of ΔE_d and σ_d are found to be (1.09 ± 0.01) eV and (2.39 ± 0.02) × 10^{-9} Ω^{-1}cm^{-1} at 295 K respectively.

Fig. 8 shows the temperature dependence of photo conductivity (σ_{ph}). It is clear from the figure that the photoconductivity is an activated process and the activation energy (ΔE_{ph}) for photoconduction is much smaller than dark conduction. The value of photo activation energy has been calculated from the slope of the curve of Fig. 8. The values of ΔE_{ph} and σ_{ph} are found to be (0.44 ± 0.01) eV and (7.72 ± 0.02) × 10^{-8} Ω^{-1}cm^{-1} at 295 K respectively. It is also clear from the figure that no maximum in the steady state photoconductivity with temperature has been observed in the measured temperature range.

Intensity dependence of steady state photoconductivity has also been studied to see the nature of recombination processes. The plot of $\ln\sigma_{ph}$ vs lnF is straight line as shown in Fig. 9, which indicate that the photoconductivity (σ_{ph}) follows a power law with intensity (F) i.e.

$$\sigma_{ph} \propto F^{\gamma} \tag{9}$$

where $0.5 \leq \gamma \leq 1.0$. According to Rose [26], the value of γ between 0.5 and 1.0 can not be understood by assuming a set of discrete trap levels but considering the existence of continuous distributions of trap levels in the band gap. In n-SeSn thin film, the value of γ is found to be 0.62, which indicate that a continuous distribution of localized states exists in the mobility gap of the present material and the resulting recombination mechanism will be bimolecular [26], where the recombination rate of electrons is proportional to the number of holes.

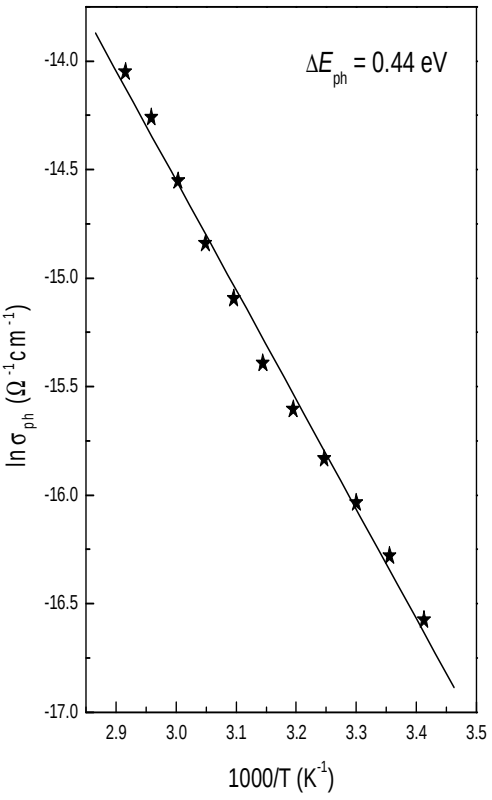

Fig. 8. Temperature dependence of photo conductivity for n-SnSe thin film.

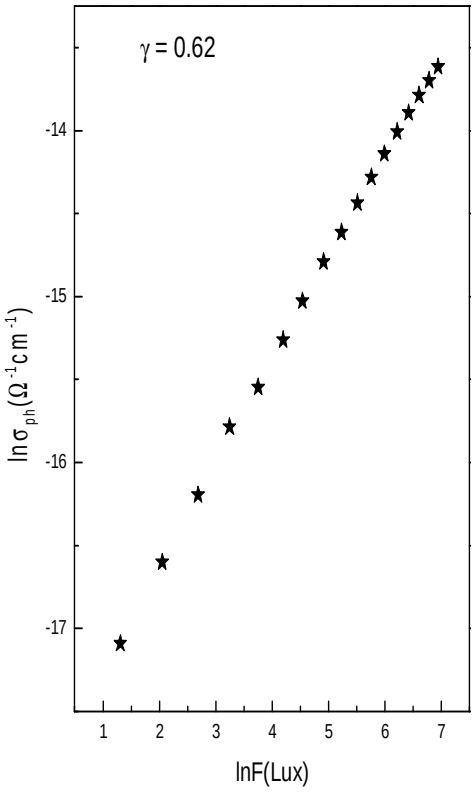

Fig. 9. Intensity dependence of photo conductivity for n-SnSe thin film.

3.2.2 Transient photoconductivity

Fig. 10 shows the rise and decay of photocurrent at room temperature (295 K). It is clear from the figure that the photocurrent first rises and then settles down to a steady state value which is slightly lower than the initial value. It is also observed that the decay of photocurrent is quite slow and a persistent photocurrent is observed. It is believed that the persistent photocurrent may not be simply due to carriers trapped in the localized states [27]. So, for simplifying the analysis, the persistent photocurrent is subtracted from the measured photocurrent

In the present case, these decay curves are not having same slope but the slope goes on decreasing continuously as the time of decay increases (result not shown here). This indicates that

the traps are present at all the energies in the band gap. These traps have different time constant and hence giving the non-exponential decay of photoconductivity. In materials, having traps in the mobility gap, the recombination time of carriers is same as the carrier life time when the free carrier density is more than the trapped carrier density [28]. If the free carrier density is much less than the trapped carriers, then the recombination process is dominated by the rate of trap emptying and is much larger than the carrier life time, resulting in a slow decay.

The density of thin films is known to decrease due to the presence of a large number of defects, which are simulated as voids using the EMA [29]. Simultaneously, the reduction in particle size leads to an increased level of disorder in the system. This is understandable since a reduction in the grain size results in a larger fraction of atoms residing at the grain boundaries than with in the grain. With the presence of voids, the extent of defects like dangling bonds present in the surface should lead to a slow decay of photocurrent.

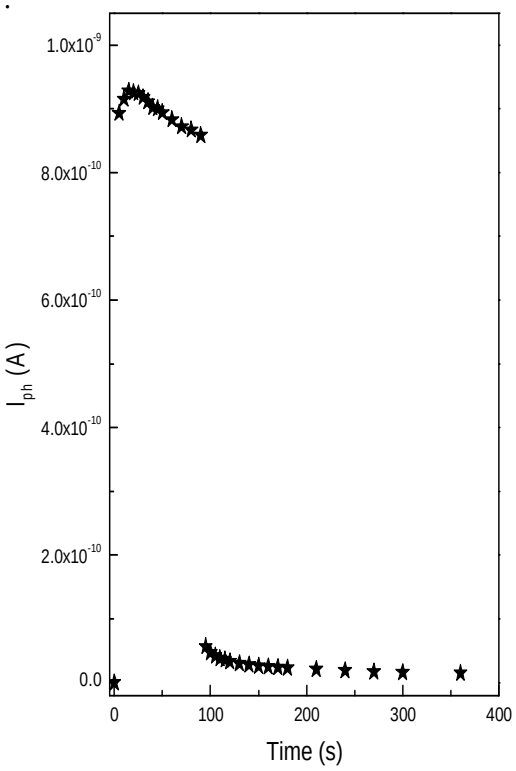

Fig. 10. Rise and decay of photocurrent for n-SnSe thin film.

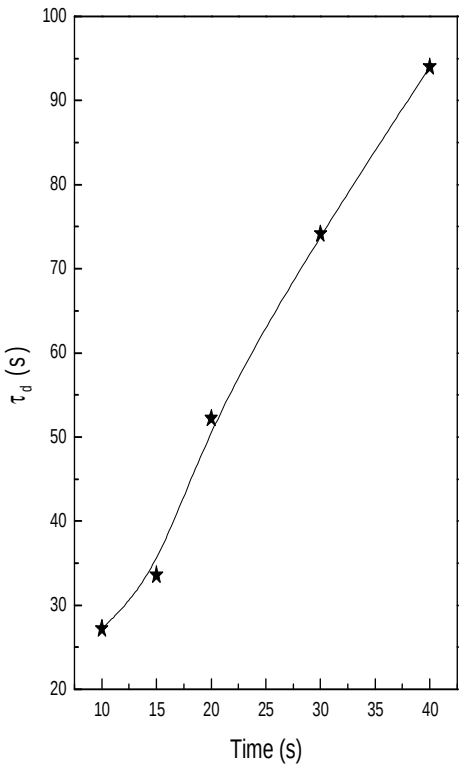

Fig. 11. τ_d as a function of time during decay of photocurrent.

To study the decay rate analysis quantitatively, the decay time constant [30] has been calculated using relation:

$$\tau_d = -\left[\frac{1}{I_{ph}}\left(\frac{dI_{ph}}{dt}\right)\right]^{-1} \tag{10}$$

where I_{ph} is the maximum photocurrent at t = 0 for a given applied voltage. From the slopes of I_{ph} vs time curve, we have calculated the values of τ_d using equation (10) at various times of the decay curve of figure 10. Fig. 11 shows the plot of τ_d vs time at a temperature 295 K and at intensity 1035 Lux. It is clear from the figure that the decay constant increases with time, which confirms the non-exponential decay of photocurrent. For exponential decay, the decay constant should not vary

with time. The slow decay process observed in the n-SnSe thin film samples is due to the presence of the deep localised states in this material.

4. Conclusions

Thin films of n-SnSe have been prepared by the thermal evaporation technique at low partial pressure of Ar gas. A blue shift in the fundamental edge has been observed due to the reduction in the particle size. The observed blue shift in the absorption edge may be due to the outcome of confinement effects. Band gap value increases to (2.18 ± 0.01) eV as compared to the bulk value (1.68 ± 0.01) eV. From the band gap shift, diameter of the nanocrystallites have been calculated and found to be ~ 3 nm. Steady state photoconductivity studies indicate that there is a continuous distribution of localised states. Decay of photocurrent is slow and it is found that the deeper localised states are present in this material.

Acknowledgements

This work is financially supported by the C.S.I.R. (major project), New Delhi. GS and AT are grateful to UGC and CSIR, New Delhi respectively for providing financial assistance.

References

[1] B. Pejova, I. Grozdanova, Mat. Chem. Phys. **90**, 35 (2005).
[2] V. C. Costa, Y. Shen, K. L. Bray, J. Non-Cryst. Solids **304**, 217 (2002).
[3] S. N. Sarangi, S. N. Sahu, Physica E **23**, 459 (2004).
[4] U. V. Desnica, I. D. Desnica-Frankovic, O. Gamulin, C. W. White, E. Sonder, R. A. Zuhr, J. Non-Cryst. Solids **299**, 1100 (2002).
[5] L. Li, J. Hu, W. Yang, A. P. Alivisatos, Nano Letters **1**, 349 (2001).
[6] L. E. Bruce, J. Chem. Phys. **80**, 4403(1984).
[7] Z. Zhang, M. Zhao, Q. Jiang, Semicond. Sci. Technol. **16**, L33 (2001).
[8] S. B. Qadri, E. F. Skelton, D. Hsu, A. D. Dinsmore, J. Yang, H. F. Gray, B. R. Ratna, Phys. Rev. B **60**, 9191 (1999).
[9] C. C. Chen, A. B. Herhold, C. S. Johnson, A. P. Alivisators, Science **276**, 398 (1997).
[10] P. Nemec, D. Mikes, J. Rohovec, E. Uhlirova, F. Trojanek, P. Maly, Mat. Sci. Eng. B **69**, 500 (2000).
[11] J. F. Suyver, R. Bakker, A. Meijerink, J. J. Kelly, Phys. Stat. Sol. (b) **224**, 307 (2001).
[12] D. L. Kelin, R. Roth, A. K. L. Lim, A. P. Alivisatos, P. L. McEuen, Nature **389**, 699 (1997).
[13] K. R. Murali, V. Swaminathan, D. C. Trivedi, Sol. Energy Mat. Sol. Cells **81**, 113 (2004).
[14] E. Nogales, B. Mendez, J. Piqueras, R. Plugaru, Semicond. Sci. Tech. **16**, 789 (2001).
[15] P. Vasa, P. Taneja, P. Ayyub, B. P. Singh, R. Banerjee, J. Phys.: Condens. Matter **14**, 281 (2002).
[16] V. Nikfim, P. A. Crowell, J. A. Gupta, D. D. Awschalom, F. Flack, N. Samarth, Appl. Phys. Lett. **71**, 1213 (1997).
[17] M. Tanaka, A. Sawai, M. M. Sengoku, M. Kato, Y. Masumoto, J. Appl. Phys. **87**, 8535 (2000).
[18] A. Thakur, V. Sharma, G. S. S. Saini, N. Goyal, S. K. Tripathi, J. Phys D.: Appl. Phys. **38**, (2005) (In press).
[19] J.N. Hodgson, Optical Absorption and Dispersion in Solids, London: Chapman and Hall (1970)
[20] Z. Ynping, Z. Chuang, G. Xinshi, L. Xingang, J. Phys. D: Appl. Phys. **25**, 1004(1992).
[21] J. I. Pankove, Optical Processes in Semiconductors, Englewood Cliffs. NJ: Prentice-Hall (1971).

[22] A. Efros, A. L. Efros, Sov. Phys. Semicond. **16**, 772 (1982).
[23] W. Wei-Yu, J. N. Schulman, T. Y. Hsu, Feron Uzi, Appl. Phys. Lett. **51**, 710 (1987).
[24] S. Hayashi, K. Yamamoto, J. Phys. Soc. Japan **56**, 2229 (1987).
[25] S. Chandra, S. T. Sundari, G. Raghavan, A. K. Tyagi, J. Phys. D: Appl. Phys. **36**, 2121 (2003).
[26] A. Rose, Concept in Photoconductivity, New York: Interscience, (1963).
[27] V. Sharma, A. Thakur, P. S. Chandel, N. Goyal, G. S. S. Saini, S. K. Tripathi, J. Optoelectron. Adv. Mater. **5**, 1243 (2003).
[28] M. Igalson, Solid State Commun. **44**, 44 (1982).
[29] G. W. Mbsie, D. Le. Bellac, G. A. Niklasson, C. G. Granvist, J. Phys. D: Appl. Phys. **30**, 2103 (1997).
[30] W. Fuhs, D. Meyer, Phys. Stat. Solidi (a) **24**, 2754 (1974).